Environmental Modelling & Software 88 (2017) 1–9

Contents lists available at ScienceDirect

Environmental Modelling & Software

journal homepage: www.elsevier.com/locate/envsoft

Role of rainstorm intensity underestimated by data-derived flood models: Emerging global evidence from subsurface-dominated watersheds

Nick A. Chappell [a, *], Tim D. Jones [a], Wlodek Tych [a], Jagdish Krishnaswamy [b]

[a] Lancaster Environment Centre, Lancaster University, Lancaster, UK
[b] Ashoka Trust for Research in Ecology and the Environment (ATREE), Bangalore 560064, India

A R T I C L E I N F O

Article history:
Received 29 February 2016
Received in revised form
26 October 2016
Accepted 27 October 2016
Available online 16 November 2016

Keywords:
Rainfall intensity
Storm hydrograph
Transfer function
Flood
Nonlinearity

A B S T R A C T

Intense rainstorms are a prevalent feature of current weather. Evidence is presented showing that simulation of flood hydrographs shown to be dominated by subsurface flow requires watershed model parameterisation to vary between periods of different rainstorm intensity, in addition to varying with antecedent basin storage. The data show an emerging global relation between flood response and the intensity of rainstorms. Flood responses are quantified as watershed residence times (strictly time constants of nonlinear transfer-function models) identified directly from information contained within 15-min rainfall and streamflow observations. The emerging monotonic, curvilinear relation indicates that (subsurface) watershed residence time decreases as mean intensity rises, and is seen over a wide range of synoptic conditions from temperate and tropical climates. Projected increases in rainstorm intensity would then result in a greater likelihood of river floods in subsurface-dominated watersheds than is currently simulated by systems models omitting this additional nonlinearity.

Software availability

Program title: CAPTAIN
Developers: Peter Young, Wlodek Tych, Diego Pedregal, James Taylor and Paul McKenna (Lancaster University) Contact e-mail: p.young@lancaster.ac.uk or c.taylor@lancaster.ac.uk
First available: February 2004 (Version 5 released on Internet)
Hardware: PC platforms supporting Matlab™
Software: Captain Toolbox for Matlab™: download from http://www.lancaster.ac.uk/staff/taylorcj/tdc/download.php
Toolbox requirements: Most of the functionality is available using the basic Matlab package

1. Introduction

Drainage basins temporarily store each pulse of rainfall to give a streamflow output more damped than that of the rainfall input. With physics-based watershed models the damping is produced primarily by combination of the prevailing antecedent moisture states with the unsaturated permeability distributions (Bear et al., 1968; Ali et al., 2012). With systems models of basins the damping in the rainfall (r) or effective rainfall (r_{eff}) to streamflow (q) signal is often quantified using residence times (or time constants) of a transfer-function or impulse-response function (Young, 1998; Box et al., 2008). The r_{eff} is the rainfall signal after a nonlinear transformation to account for the effects of antecedent watershed storage on hydrograph response (e.g., Whitehead et al., 1979; Young and Beven, 1994; Ye et al., 1998; McIntyre et al., 2011).

There is a general perception that stream hydrographs are flashier and more likely to produce over-bank flows in periods and/or regions experiencing more intense rainfall events. A very small number of studies have demonstrated an apparent link between the properties of hydrograph shape and averaged rainfall intensity characteristics for a specific storm period. Minshall (1960) showed that different measures of the shape of calculated Unit Hydrographs (Sherman, 1932) altered with changes in the hourly rainfall intensity (inches/h) averaged over individual storms. As a specific example, this study showed that the time for the hydrograph to recess to 40 percent of the peak-flow reduced as the average hourly

* Corresponding author. Lancaster Environment Centre, Lancaster University, Lancaster LA1 4YQ, UK.
E-mail address: n.chappell@lancaster.ac.uk (N.A. Chappell).

http://dx.doi.org/10.1016/j.envsoft.2016.10.009

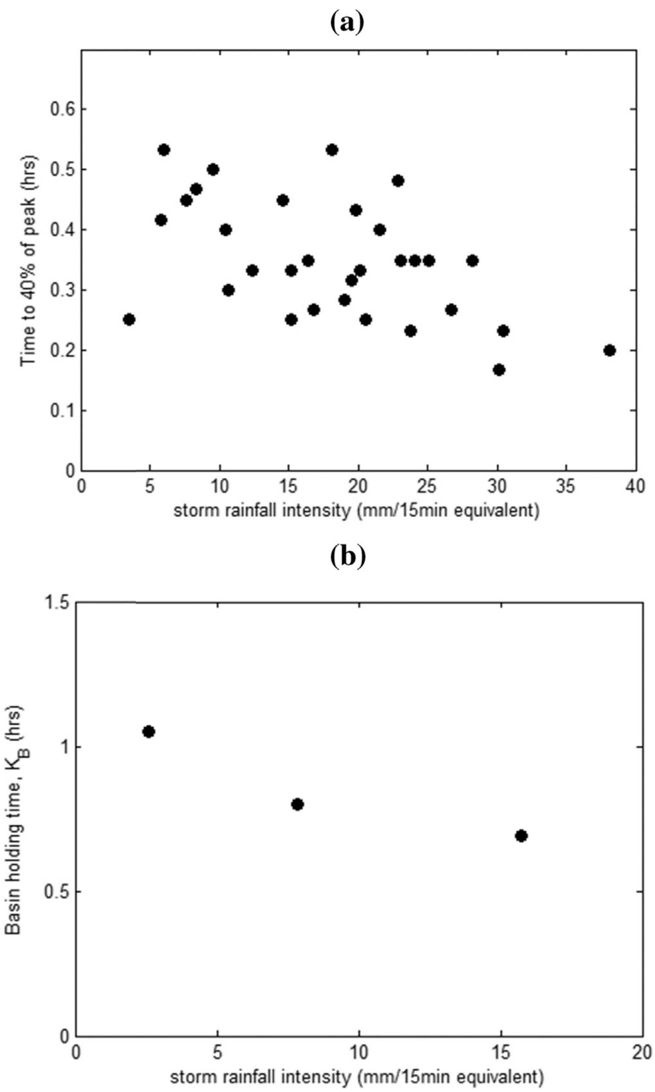

Fig. 1. Relationship of measures of hydrograph shape with rainfall intensity averaged over a storm period from two previous studies. (a) Time from the Unit Hydrograph peak to the 'point on the streamflow recession at 40% of the peak' against rainfall intensity (inches/h) averaged over the specific storm (converted to mm/15min equivalent), adapted from Table 3 in Minshall (1960). (b) Basin 'holding time' of the Instantaneous Unit Hydrograph against rainfall intensity (cm/h) averaged over the specific storm (converted to mm/15min equivalent), adapted from Fig. 6 in Wang et al. (1981).

storm rainfall intensity increased (Fig. 1a). Similarly, Wang et al. (1981) showed that the basin 'holding time' (K_B) reduced as the average hourly storm rainfall intensity (inches/h) increased (Fig. 1b). In other words, change in hyetograph shape (i.e., temporal evolution of rainfall totals through a storm) between different types of storm can produce different hydrograph shapes and hence nonlinearity in the rainfall to streamflow response (Rodríguez-Iturbe et al., 1982).

Several studies undertaken in regions with more intense tropical rainfall events (e.g., Noguchi et al., 1997; Chappell et al., 2006, 2012; Hugenschmidt et al., 2014) have demonstrated that very flashy stream hydrographs can be produced almost entirely from subsurface flow pathways, i.e., without the need for activation of significant volumes of overland flow (on slopes) during storms. Consequently, nonlinear rainfall-streamflow response generated in such basins would be entirely related to shallow or deeper groundwater flow pathways. Even after correcting for the widely acknowledged nonlinear effects of antecedent wetness on rates of subsurface flow (Graham et al., 2010), it is *our research hypothesis that additional nonlinearities in rainfall-streamflow response dominated only by subsurface flow may be generated by changes in hyetograph shape*. If this hypothesis is valid, it would require explicit model parameterisation or temporal shifts in existing systems model parameterisations to represent and so better simulate streamflow through storms with contrasting conditions. The rainfall intensity regime for a period of contiguous storms is likely to vary with synoptic meteorological typology in time and across the globe. Those in the tropics tend to have greater intensities than those prevailing in temperate regions primarily due to differences in regional convection (Wohl et al., 2012). Equally large variations are seen within the tropics; for example synoptic conditions associated with tropical cyclones tend to have greater average intensities than those associated with local thunderstorms (Francis and Gadgil, 2006; Zipser et al., 2006; Shepherd et al., 2007). To reiterate, non-stationarity in systems model parameters (see e.g., Kundzewicz and Napiórkowski, 1986) characterising rainfall-streamflow responses in subsurface-flow dominated watersheds caused by temporal variations in rainfall intensity regime, would be in addition to those caused by changes in antecedent moisture (or seen in basins with overland flow activation).

While previous studies provide some observational evidence for the potential effects of storm-averaged rainfall intensity on the non-stationarity of hydrograph residence times (Fig. 1ab), the absence of a generic numerical relationship (for basins dominated only by subsurface flow) may be responsible for the lack of a wider recognition of the phenomenon. In part this may be due to the limited range of hydrograph responses and storm-types examined previously (see e.g., Minshall, 1960; Wang et al., 1981; Rodríguez-Iturbe et al., 1982). Consequently, a greater diversity of synoptic meteorological conditions was examined in this study to attempt to *quantify the first approximation of a generic relationship between rainfall intensity characteristics and storm hydrograph shape for subsurface-dominated flood responses.*

2. Experimental data sets

In this study selected rainfall and streamflow records were those associated with a set of experimental basin systems (each <5 km^2) known to be dominated by shallow subsurface paths (sometimes called 'interflow'), in addition to experiencing a broad spectrum of synoptic conditions. One such system is the South Creek basin in a humid tropical region of Australia (e.g., Chappell et al., 2012). Two other example experimental basins in the tropics (Fig. 2) with hydrograph responses shown to be dominated by shallow subsurface paths, are the Baru basin on Borneo Island (e.g., Kretzschmar et al., 2014) and Saimane basin of the larger Aghanashini basin in India (Bonell et al., 2010; Krishnaswamy et al., 2012). These have contrasting rainfall intensity regimes, with the Baru being dominated by local thunderstorms and Saimane by Tropical Convergence Zone (TCZ) events in the summer monsoon. To capture the effects of typically lower intensity rain-events in temperate regions, three basins from across upland UK are incorporated in the analysis (Fig. 2). The Hafren, Greenholes and Nant-y-Craflwyn basins are dominated by shallow water-paths (Bell, 2005; Chappell and Lancaster, 2007; Jones and Chappell, 2014) and frontal rainfall. Further basin details are given in Table 1. While rainfall-streamflow responses for only six experimental basins are studied, the 16 periods of contiguous storms analysed do cover a diverse range of synoptic conditions (Table 2).

The primary hyetograph characteristic evaluated was the average rainfall depth from all 15-min intervals with measured rainfall in the selected periods of contiguous storms of the same

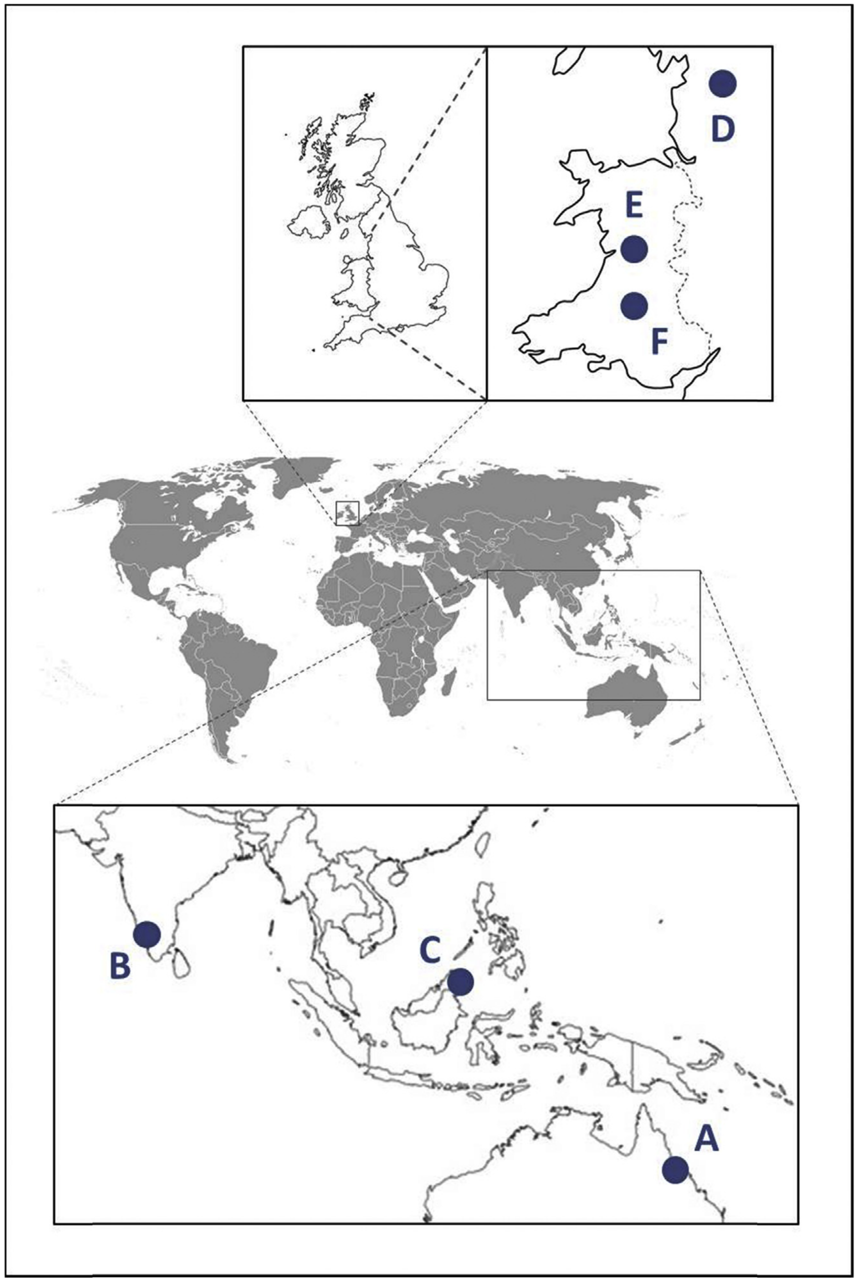

Fig. 2. Geographic locations of the experimental basins detailed in Table 1. Location A is the South Creek basin in tropical Queensland, Australia; location B is the Saimane basin in the Western Ghats mountains in Karnataka state of India; location C is the Baru basin in Sabah state of Malaysia on Borneo Island; location D is the Greenholes basin in temperate northwest England, United Kingdom; and locations E and F are the Hafren basin and Nant-y-Craflwyn basin, respectively, in mid-Wales, United Kingdom.

synoptic type (I_{WET15}). Thus 15-min periods recording zero rainfall were excluded from the statistics. This removed the confounding influence of differing durations of dry spells within the selected period of contiguous storms on the calculated rainfall characteristic. This also allows for storms of different duration to be characterised (Brommer et al., 2007). A total of 16 separate periods covering a diverse range of synoptic conditions were selected (Table 2).

For the South Creek basin the periods covered are: tropical cyclone 'Ivor'; part of the post-monsoon period; part of the Australian monsoon (December–March); and localized convective events (Klingaman, 2012). The southwest summer monsoon in India comprises of several 'active phases' caused by distinct synoptic systems that may have differing rainfall characteristics (Francis and Gadgil, 2006). Consequently, for the Saimane basin in India, periods comprising of different active phases within the 2013 monsoon, were selected for the modelling. For the Baru basin on Borneo Island, periods of localized convective rainfall (Bidin and Chappell, 2006) were selected for comparison. For a few 15-min sampling increments within the tropical data sets, rainfall intensities were very high, reaching a maximum of 29.25 mm/15min (Supplementary Material Fig. S4ab). This maximum value is equivalent to more than 7 tips per minute of the 0.25 mm/tip tipping-bucket raingauge (Mark II Rimco) used at the South Creek basin (Gilmour et al., 1980). The 15-min sampling increments with such high rainfall intensities are likely to give under-estimates of

Table 1
Characteristics of the experimental basins selected to provide the data sets for the 16 periods of contiguous storms.

Experimental basin	Name of the period of contiguous storms	Basin area (km^2)[b]	Stream order: Strahler method[g]	Dominant soil type	Surficial geology	Solid geology	Land cover
South Creek, Australia[a]	Periods 1 to 4	0.3	4	Acrisol	>6 m weathered rock	Basic metamorphic	Tropical evergreen forest (disturbed mesophyll vine forest)
Saimane, India[b]	Periods 5 to 8	4.9	3	Nitosol	1-10 m weathered rock	Metamorphic	Tropical evergreen forest (disturbed with agroforestry)
Baru, Malaysia[c]	Periods 9 to 10	0.4	3	Alisol	<3 m weathered rock	Melange	Tropical evergreen forest (disturbed lowland dipterocarp)
Greenholes, UK[d]	Periods 11 to 12	1.1	2	Gleysol	1 to >4 m glacial till	Sedimentary (Carboniferous)	Grassland (heather moorland and improved pasture)
Hafren, UK[e]	Periods 12 to 14	3.7	2	Histosol & Podzol	0.1 to ≥10 m solifluction deposit	Metamorphic (Silurian)	Plantation (conifer) & grassland (heather moorland)
Nant-y-Craflwyn, UK[f]	Periods 15 to 16	0.5	2	Gleysol & Podzol	1-5 m glacial till	Metamorphic (Ordovician)	Plantation (conifer)

[a] Gilmour et al. (1980), Chappell et al. (2012).
[b] FAO UNESCO (2004), Bonell et al. (2010), Krishnaswamy et al. (2012).
[c] Chappell et al. (1999, 2012).
[d] Chappell and Lancaster (2007).
[e] Newson (1976).
[f] Reynolds and Norris (1990), Jones and Chappell (2014).
[g] Gregory and Walling (1973).

Table 2
Characteristics of the sixteen study periods and models of effective rainfall to streamflow response identified by the RIVC algorithm.

Period	Regime[a,b]	Experimental basin	$I_{WET15eff}$[c] (mm/15-min)	Model[d]	R_t^2 [e]	TC_{fast} (hrs)[f]	*fast%*[g]
1	1 (Aw)	South Creek	2.0705	[2 2 0]	0.931	0.286 ± 0.004	50.8 ± 10
2	2 (Aw)	South Creek	1.5656	[2 2 0]	0.855	0.116 ± 0.001	63.3 ± 9.4
3	3 (Aw)	South Creek	2.0411	[2 2 0]	0.898	0.358 ± 0.002	40.6 ± 3.7
4	4 (Aw)	South Creek	0.8721	[2 2 0]	0.803	1.360 ± 0.003	19.7 ± 11
5	5 (Am)	Saimane	2.1868	[2 2 0]	0.777	0.355 ± 0.101	59.3 ± 38
6	5 (Am)	Saimane	0.9733	[2 2 0]	0.892	0.444 ± 0.014	37.3 ± 15
7	5 (Am)	Saimane	0.7374	[2 2 1]	0.944	0.578 ± 0.024	32.5 ± 14
8	5 (Am)	Saimane	1.2920	[2 2 0]	0.929	0.270 ± 0.023	46.1 ± 19
9	4 (Af)	Baru	0.7159	[2 2 0]	0.927	1.702 ± 0.001	65.5 ± 44
10	4 (Af)	Baru	1.3246	[2 2 1]	0.884	0.830 ± 0.005	65.4 ± 19
11	6 (Cfb)	Greenholes	0.6167	[2 2 0]	0.958	4.605 ± 0.076	74.6 ± 9.2
12	6 (Cfb)	Greenholes	0.7615	[2 2 1]	0.902	2.645 ± 0.043	55.7 ± 6.3
13	6 (Cfb)	Hafren	0.7240	[2 2 3]	0.985	1.375 ± 0.023	42.1 ± 7.4
14	6 (Cfb)	Hafren	0.4822	[2 2 0]	0.947	1.869 ± 0.017	25.8 ± 8.1
15	6 (Cfb)	Nant-y-Craflwyn	0.4831	[2 2 2]	0.966	3.209 ± 0.355	52.9 ± 26
16	6 (Cfb)	Nant-y-Craflwyn	0.3305	[2 2 1]	0.961	3.581 ± 0.038	66.3 ± 9.2

[a] Storm-type characterizing the regime in period: 1 Tropical cyclone Ivor, 2 post-monsoon period, 3 monsoon period, 4 convective events, 5 Tropical Convergence Zone event, 6 frontal rainfall event.
[b] Köppen-Geiger climate regime: Aw = tropical wet and dry climate, Am = tropical monsoon climate, Af = tropical rainforest climate, Cfb = oceanic climate (Peel et al., 2007).
[c] Average effective rainfall from all 15-min intervals in the selected period receiving rainfall.
[d] Model structure is given as the number of [Denominators, Numerators, Pure Time Delays] as in Chappell et al. (2012).
[e] R_t^2 is the simulation efficiency defined as the variance in the model residuals normalised by the variance in the observed streamflow data.
[f] TC_{fast} is the Dynamic Response Component (DRC) of the time constant of the fast response component.
[g] *Fast%* is the DRC of the percentage of response following the fast component (e.g., Jones and Chappell, 2014). Uncertainty in the TC_{fast} and *fast%* values is twice the standard deviation derived from 1000 Monte Carlo realizations using uncertainty information implicit to the RIVC method.

the true 15-min totals (Saidi et al., 2014). Such high intensities are, however, limited to very few increments within the records, and so have little impact on statistics averaged across the periods of contiguous storms. The periods of contiguous storms selected for modelling temperate basins all received rainfall from frontal systems that were expected (Little et al., 2008) and shown (Supplementary Material Fig. S4ab) to have lower mean intensity values. In temperate UK, intense rainfall exceeds 4 mm/h, equivalent to 1 mm/15-min. Consequently, for the study basins in both temperate and tropical regions with a range in I_{WET15} less than 1 mm/15-min, two periods contrasting in rainfall intensity were selected, while for those with a larger range four contrasting periods were used. The rainfall intensity statistic was also calculated for the effective rainfall to be used in the r_{eff}-q modelling (i.e., modelling once the effects of antecedent conditions removed), to give $I_{WET15eff}$.

3. Model identification methods

The Refined Instrumental Variable in Continuous-time (RIVC) algorithm (Young and Jakeman, 1979; Young and Garnier, 2006; Young, 2015) was used to capture the dominant modes of r_{eff}-q response of each period to compare with the $I_{WET15eff}$ statistic. Historically, most rainfall-streamflow models based on transfer functions (TFs) have been discrete-time dynamic models. Discrete-time dynamic models describe a system using difference equations e.g., $q(k) = ar(k\text{-}1)$, where a is a recession term and $r(k\text{-}1)$ represents the rainfall input at the previous kth sampling time. In contrast, continuous-time dynamic models describe a system using differential equations (Young, 2015). These models are generally more difficult to estimate, but produce more reliable model parameter estimates where the system dynamics are very fast, i.e., where the dynamics are nearly as fast as the sampling increments in the data. Given the likelihood of short residence times for some of the rainfall-streamflow responses in the selected tropical basins (Chappell et al., 2012), a continuous-time modelling approach was used in this study.

The RIVC algorithm was used to identify model structures and parameters following a three-stage Data-Based Mechanistic (DBM) approach. The first stage of this approach is to apply a large range of mathematical relationships that might capture the dynamics of the streamflow from the rainfall or effective rainfall. Thus the model structures identified are based on those that can describe the dynamics between the observed input data and observed output data; hence the models can be defined as *data-based.* This first stage is undertaken without making any *a priori* assumptions about the nature of the processes within the subsurface flow system. It also involves the identification and separate parameterisation of the nonlinear effects on the rainfall-streamflow response caused by changing antecedent subsurface storage between the simulated periods via transformation of rainfall to effective rainfall (Young and Beven, 1994; Chappell et al., 2012; Kretzschmar et al., 2014). The second stage of the DBM approach involves the rejection of as many of the identified models as possible based upon mathematical-statistical criteria. This involves model rejection based upon: 1/an unacceptable degree of correspondence between the observed and simulated streamflow (i.e., poor simulation efficiency), 2/an unacceptable degree of model over-parameterisation (i.e., rejection of models that are more complex than can be warranted by the information contained in the observations), and 3/the failure of various mathematical diagnostic checks, e.g., models exhibiting unstable behaviour. The third and final stage of the approach is the rejection of mathematically acceptable DBM models that do not have a feasible *hydrological process interpretation*. For example, a DBM model of streamflow that is a combination of one water-pathway that adds water to the stream and one that removes it, may be valid statistically, but is not considered consistent with perceptual models of streamflow generation systems. DBM models accepted as having a hydrological interpretation can then be defined as *mechanistic* and therefore, described as data-based mechanistic models.

The DBM approach combined with the RIVC algorithm was used for two principal reasons. First, the constraint on model structural complexity implicit within the DBM approach (so called 'model parsimony') limits the range of possible values of each parameter describing hydrograph shape, notably the α parameter(s) (Eq. (1)), thereby reducing its/their parametric uncertainty (Young, 2013). This allows differences in model parameter values between periods to be identified above the uncertainties and so permits a greater degree of process interpretation (Jones et al., 2014). Secondly, it provides an objective method for separating the effects of antecedent subsurface wetness (that are well known) from the effects of storm-period rainfall intensity on the subsurface response. Without an understanding of how storm-period rainfall intensity affects subsurface flow mechanisms directly, it would not be clear how to modify the structure of a physics-based model to simulate this hypothesised phenomenon. The need for mechanistic (or process) interpretation of all DBM models, combined with their acknowledged parsimony, means that they are considered to be a state-of-the-art approach for gaining process understanding of rainfall-streamflow systems (Beven, 2012; Young, 2013; Jones et al., 2014; Beven and Smith, 2014).

It is the derived RIVC transfer function parameter of the time constant (*TC* or the watershed's residence time of response derived directly from the α parameter) that translates an effective hyetograph to a hydrograph (Young, 1998; Box et al., 2008). For streamflow generation systems lacking more than a few percent of overland flow, the steepest parts of the hydrograph recession (and associated shortest *TC* identified) can be interpreted as the rapid response through the soil-water system (Barnes, 1939), i.e., shallow subsurface flow or 'interflow' pathway. Periods of contiguous storms were selected for the r_{eff}-q modelling (and associated $I_{WE\text{-}T15eff}$ determination) to give more reliable parameter estimates than can be achieved for single events with their smaller information content (see Seibert and Beven, 2009).

To capture the nonlinear effects arising from different soil moisture storages at the start of each period of observations, the rainfall observations for each period were first filtered to give r_{eff} (rather than r) using an additional, optimized model parameter, p, following Chappell et al. (2012) and Kretzschmar et al. (2014). Additional temperature modulation effects on the nonlinearity term (see e.g., Young and Beven, 1994) were not included. The sensitivity of the r_{eff}-q model to the p-value was estimated with 1000 Monte Carlo realizations of p over the range 0–1.5 (Supplementary Material Fig. S6).

The RIVC algorithm is available in the CAPTAIN Toolbox for Matlab™ (Taylor et al., 2007). Technically, it implements an iterative Instrumental Variable method for estimation of general transfer-functions that capture the dynamic relationship between the r_{eff} input and streamflow output variables using rational polynomial equations in operator s in continuous time (Eq. (1), Young, 2015). These can be directly translated in to differential equations forced by r_{eff} (Eq. (2), see e.g., Jones et al., 2014). To emphasise, the more sophisticated continuous-time version of the algorithm was used as it is less sensitive to the adverse effects of under-sampling of flashy tropical systems, compared to the discrete-time versions in CAPTAIN (i.e., RIVD, e.g., Littlewood and Croke, 2013). The risk of under-sampling effects were further reduced by utilizing rainfall and streamflow observations with a 15-min resolution (Jones et al., 2014). The Instrumental Variables (IVs) are the initial estimates of model output that permit unbiased estimation of the model parameters (i.e., α_1, α_2, β_0, β_1 and τ in Eq. (2)). These IVs, along with variables r_{eff} and q, are then used within Normal Equations to derive the parameter estimates and their covariance matrices (Young, 2015). Model structure is presented as a 'triad' of denominator-numerator-delay within square parentheses, indicating the number of denominator parameters, *den* (α_1 and α_2 parameters in the lower part of the transfer function equation), the number of numerator parameters, *num* (β_0 and β_1 parameters in the upper part of the transfer function equation) and the number of pure time delays, *delay* or τ. The form of the model with a second-order [2 2 τ] structure as an example, can be stated in continuous-time transfer-function form, as:

$$q = \left(\frac{\beta_0 s + \beta_1}{s^2 + \alpha_1 s + \alpha_2}\right) e^{-s\tau} r_{eff} \;\; ; \;\; s \sim \frac{d}{dt} \tag{1}$$

where q is the streamflow (mm/15-min), r_{eff} is the effective rainfall (mm/15-min), τ is the pure time delay between r_{eff} and an initial q response (given in number of 15-min intervals), α_1 and α_2 the parameters capturing the rate of soil-water exhaustion or residence time (/15-min), β_0 and β_1 the parameters capturing the magnitude of streamflow gain (mm q/mm r_{eff}), t is time in 15-min periods, and s is the Laplace operator (Young, 2015). Alternatively, the model can be expressed in ordinary differential equation terms (ignoring initial conditions):

$$\frac{d^2 q(t)}{dt^2} + \alpha_1 \frac{dq(t)}{dt} + \alpha_2 q(t) = \beta_0 \frac{dr_{eff}(t-\tau)}{dt} + \beta_1 r_{eff}(t-\tau) \tag{2}$$

To allow physical interpretation, this second-order model of streamflow can be decomposed by partial fraction expansion (Jakeman et al., 1990; Young and Beven, 1994) into two parallel, first-order transfer functions:

$$q = \frac{\beta_f}{s - \alpha_f} e^{-s\tau} r_{eff} + \frac{\beta_s}{s - \alpha_s} e^{-s\tau} r_{eff} \tag{3}$$

where α_f and α_s are the values (specifically roots of the characteristic equation of the differential Eq. (2)) representing the rate of soil-water exhaustion or residence time of the fast and slow components that comprise the total streamflow generation, respectively (/15-min; see Supplementary Material Table S4), and β_f and β_s the parameters capturing the magnitude of the fast and slow flow components, respectively (mm q/mm r_{eff}). Hydrological interpretation of the behaviour of these model stores is then made after calculating the Dynamic Response Characteristics, DRCs (e.g., Jakeman et al., 1993; Jones et al., 2014) of the component transfer functions from parameters α_f, α_s, β_f, β_s and τ given in Eq. (3). These DRCs include the *TC* for each component flow pathway. For the critical fast path this is given as:

$$TC_{fast} = -\frac{\Delta t}{\alpha_f} \tag{4}$$

where Δt is the time-step in the observations (15-min). The uncertainties in the α_1, α_2, β_0, β_1 values and derived TC_{fast} values were estimated using uncertainty information implicit to the RIVC method (Young, 2015) applied in 1000 Monte Carlo realizations.

4. Results and discussion

For each of the 16 periods, 36 possible models were evaluated from first-order models with no pure time delays (i.e., [1 1 0] structure) to second-order models with 8 pure time delays (i.e., [2 2 8] structure). To capture the shape of the (total) streamflow recessions, a second-order model structure was needed for most of the 16 periods analysed and was able to simulate 77.7–98.5% of the observed dynamics (Table 2). The lower simulation efficiency for period 5 (77.7%) may have been caused by differences in the rainfall intensity regime within the period, particularly between the single larger event and the series of smaller events.

For consistency, optimal second-order models were selected for interpretation of all periods. This structure can be expressed hydrologically as two parallel water-pathways (i.e., a ‘fast’ and a ‘slow’ path) within each basin system (e.g., Jakeman et al., 1990; Jakeman and Hornberger, 1993; Young and Beven, 1994; Littlewood et al., 2007; Jones and Chappell, 2014; Jones et al., 2014). The *TC* of the fastest pathway (TC_{fast}) characterizes the shape of the hydrographs surrounding the critical periods of peak streamflow, and as such is a measure of the ‘flashiness’ of the hydrograph (Table 2). This TC_{fast} was shown to be well-defined by the RIVC approach given the narrow uncertainty in the values (Table 2). Fig. 3bd shows this narrow TC_{fast} uncertainty in period 4 and 11 as examples, together with the observed and modelled streamflow (Fig. 3ac). The results from all other modelled periods are given in the supplementary material.

Table 2 shows the $I_{WET15eff}$ values for each of the 16 periods simulated, while Fig. 4a shows the model-derived TC_{fast} values plotted against $I_{WET15eff}$. The 16 values, comprising of different periods for the same basin and different basins within contrasting climatic regimes, exhibit *shorter TCs (of the fast response component) for higher values of average rainfall intensity integrated over the 15-min intervals where rain was present* (in each period of contiguous storms). This is consistent with the findings of previous studies that

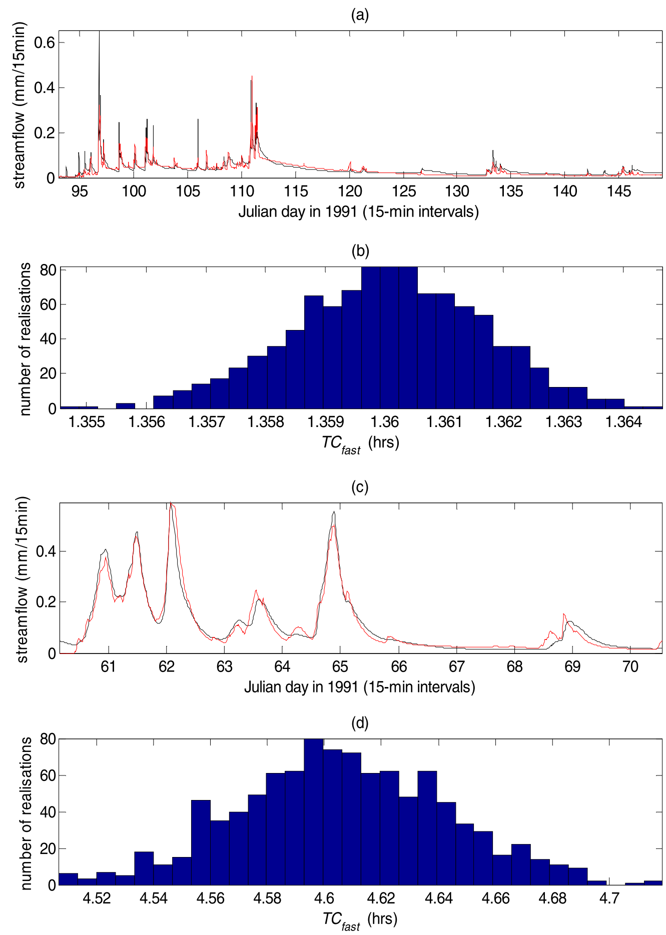

Fig. 3. Example observations and model results for period 4 (a tropical basin) and 11 (a temperate basin) shown in Table 1. (a) and (c) Observed (—) and simulated streamflow (—) for periods 4 and 11, respectively. (b) and (d) Frequency distribution of the Dynamic Response Characteristic of the TC_{fast} for periods 4 and 11, respectively, estimated using uncertainty information implicit to the RIVC method applied in 1000 Monte Carlo realizations.

have observed faster hydrograph recessions for individual storms with larger hourly rainfall intensities (see Minshall, 1960; Wang et al., 1981; Rodríguez-Iturbe et al., 1982 and Fig. 1ab). For the first time, however, we demonstrate that a strong monotonic, curvilinear relationship is apparent between TC_{fast} and $I_{WET15eff}$ for flood hydrographs dominated by subsurface flow (Fig. 4b). For clarification, this first approximation of a power law relationship was derived using the *lsqcurvefit* and *nlpredci* functions in Matlab™ on log-transformed data.

In process terms, the *TC*s of transfer-functions of subsurface-dominated r_{eff}-q systems equate to the change of basin storage within each storm, per change of streamflow generated (i.e., dS/dq). Consequently, the findings from this study would suggest that for basin systems dominated only by shallow subsurface flow, higher rainfall-intensity regimes deliver more water through the soil-water system to streams within storms rather than accumulate moisture storage within the soil. This effect becomes more pronounced with synoptic systems typically producing lower intensity rainfall, with small changes in the $I_{WET15eff}$ statistic producing large changes in the TC_{fast}. The six periods from temperate UK fall along the steeper part of the relation (Fig. 4ab), suggesting that the flashiness of frontal events in temperate streams may be more sensitive to any systematic shifts in the rainfall intensity regime

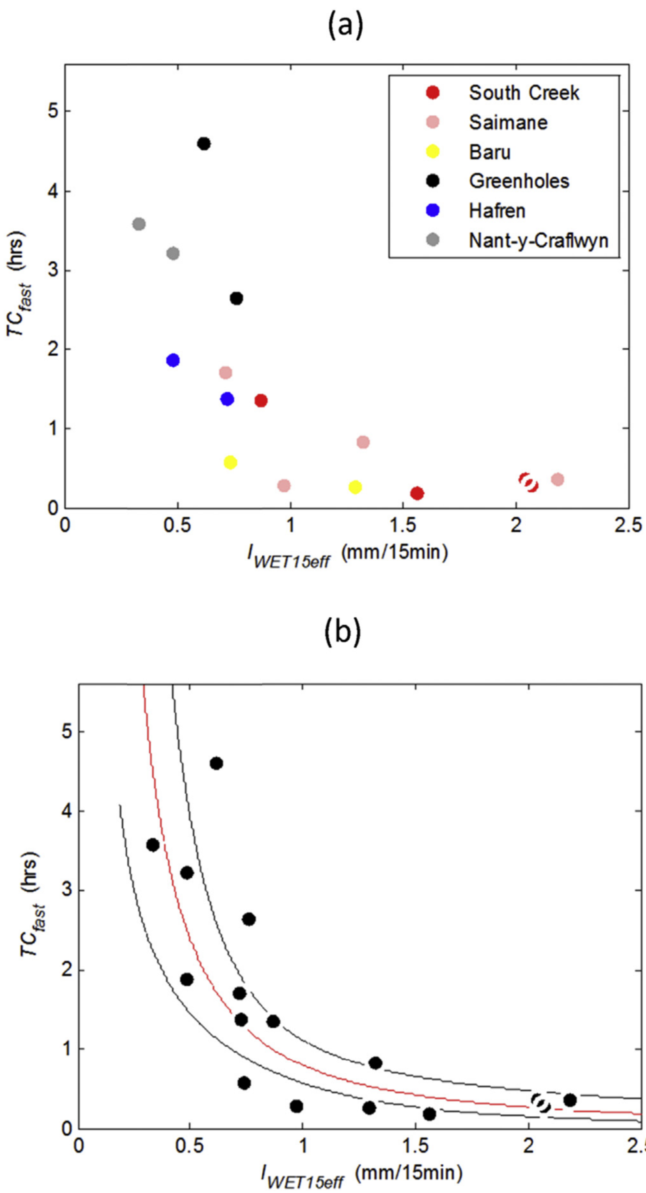

Fig. 4. Relationship between TC_{fast} and $I_{WET15eff}$ for the 16 periods of observations pooled from tropical and temperate basins. (a) Values for the same experimental basin are shown using the same colour of solid circle. The tropical basins are: South Creek, Saimane and Baru, while temperate basins are: Greenholes, Hafren and Nant-y-Craflywn. (b) The power model (Eq. (5)) and the 95% confidence intervals are shown with solid lines.

than those of basins with considerably higher rainfall intensities.

The observed relationship is given as:

$$TC_{fast} = 0.80297 I_{WET15eff}{}^{-1.568} \quad ; r^2 = 0.69 \tag{5}$$

where $I_{WET15eff}$ is the average effective rainfall integrated over the 15-min intervals with rain of the selected period of contiguous storms (mm/15min), and TC_{fast} is the associated time constant (hrs) of the fast component of a parallel decomposition of a second-order, transfer function defined by the RIVC algorithm (Fig. 4b). With this model, 69% of the variance in the TC_{fast} could be explained by the variance in the $I_{WET15eff}$ statistic for the 16 periods analysed. The relationship was tested by using the same modelling approach to derive a TC_{fast} value for a different basin during a different monitoring period. For the Nant-y-Bustach basin (UK) over a 25-day period of winter storms an $I_{WET15eff}$ value of 0.4801 mm/15min and a TC_{fast} value of 4.673 h were derived (supplementary material). The point on Fig. 4a associated with these two values lies within the 95% confidence intervals of the power model shown, and so provides some validation of the relationship. For each basin, the trend across periods affected by different intensity regimes, while less clear (Fig. 4a), was not inconsistent with the general power law observed for the whole dataset.

The same degree of explanation of the variations in the TC_{fast} was apparent if the I_{WET15} was used (Supplementary Material Fig. S10) instead of $I_{WET15eff}$ (Fig. 4b). Thus application or not of the nonlinearity transform to the rainfall data to account for the effects of antecedent basin wetness (Young and Beven, 1994) does not impact the ability to identify the relationship with hydrograph flashiness. In some contrast, a much lower degree of explanation of the variations in the TC_{fast} resulted when the median rainfall from all 15-min intervals receiving rainfall (I_{MED}) was derived for each period (Supplementary Material Fig. S11). A monotonic relationship was absent between the model parameter p capturing the non-linearities arising from the antecedent moisture conditions and the derived TC_{fast} values (Supplementary Material Fig. S12). A relationship with TC_{fast} was similarly absent with the geomorphic characteristic of basin area (Supplementary Material Fig. S13). Others have attempted to quantify the effects of rainfall intensity characteristics on the proportion of fast-flow during storms (Hewlett et al., 1977; Loague and Freeze, 1985; Bren et al., 1987); this is equivalent to the *fast%* values derived in this study and presented in Table 2. The $I_{WET15eff}$ and I_{WET15} statistic did not, however, produce any systematic relationship with the modelled *fast%* values (Supplementary Material Fig. S14). The shape of the stream hydrograph during storm-events (i.e., TC_{fast} or rainfall-streamflow ‘flashiness’) was not examined by these other studies. Furthermore, these studies identified only very weak relationships between rainfall intensity characteristics and the proportion of fast-flow during storms. Better correlations were obtained by Howard et al. (2010), but only after subdivision of the rainfall intensity data into several seasonal periods and classes.

For watersheds with subsurface-dominated storm hydrographs, values of systems model watershed parameters representing the residence time of response (i.e., TC) are not varied within the current generation of systems models because of differing synoptic storm type (and associated hyetograph shape). Only the separate effects of changing antecedent basin wetness are incorporated into systems model simulations. If watershed model parameters need to be varied between periods of differing storm-averaged intensity (i.e., $I_{WET15eff}$), as our results would suggest (from evidence initially based on subsurface-dominated systems), then models that do not do this will underestimate the fast residence times (i.e., TC_{fast}) in periods of higher than average storm intensity. This would mean that simulations of flood events caused by particularly intense storm systems in a long modelled record will be smaller than observed. Additionally, it may mean that locations where the incidence of flooding is particularly sensitive to discrete periods of higher rainstorm intensity (e.g., flooding associated with convective rainfall cells in Southern England in an otherwise frontal rainfall regime: Hand et al., 2004) may not be highlighted sufficiently.

Given that the form and parameters of the relationship are developed from only 16 data periods for initially subsurface-dominated systems, its wider global applicability requires further evaluation of the identified relationship using many combinations of geomorphic setting, as discussed in the closing remarks. The strength of the relationship identified so far is, however, surprising given the diversity of synoptic meteorological conditions (producing a wide range of rainstorm intensities) examined in this study.

As a working hypothesis, the shallow subsurface systems may be responding differently between periods of contrasting rainfall intensity as a result of activation-deactivation of parts of the soil-macropore systems. It is likely that at higher intensities in a particular basin, more of the macropore system is activated giving a disproportionate and thus nonlinear impact on the shallow subsurface flow (Weiler, 2005) and subsequent rapid loss of moisture storage to streamflow generation. The critical role of soil-macropores in streamflow generation is widely acknowledged. Field methods for their characterization for use in basin modelling does, however, remain poorly understood (Beven and Germann, 2013), thereby restricting the development of physics-based models to show their potential role in explaining the impacts of rain-event characteristics on streamflow generation.

5. Conclusions

While a hydrological theory explaining the impact of differences in hyetograph shape (i.e., time-integrated, rain-event characteristics) on hydrograph shape (by a mechanism other than overland flow) may be poorly developed, this is the first study to identify a strong quantitative relationship with rainfall intensity for flashy, subsurface only dominated systems. To reiterate, the strength of the relationship identified so far is, however, surprising given the diversity of synoptic meteorological conditions producing different hyetograph shapes examined in this study. These initial findings do need to be further evaluated (i.e., 'conditional validation': Beven and Young, 2013) against a considerably larger set of experimental basins similarly dominated by shallow subsurface flow. Equally, the presence of relationships for TC_{fast} of experimental basins with significant volumes of deep groundwater-flow (Lesack, 1993; Ockenden and Chappell, 2011) should be evaluated. Furthermore, the link between the rainfall intensity regime and the fast component of streamflow response should be studied with a systematic analysis of storm-type (see e.g., Merz and Blöschl, 2003).

If data-derived model parameters for subsurface-dominated floods need to be varied between periods of differing storm-averaged intensity (i.e., $I_{WET15eff}$), as our results would suggest, then models that do not do this may underestimate the fast residence times (i.e., TC_{fast}) in periods of higher than average storm intensity. This would mean that simulations (or long-range forecasts: Pedregal et al., 2009) of flood events caused by particularly intense storm systems in a long record will be less flashy than observed. For larger storm events, if the fast component of flow is delivered more quickly (i.e., shorter TC_{fast}), there would be a greater likelihood of floods, caused by over-bank flows, than systems models indicate. This could have profound implications for the subsequent economic and social costs of flooding globally (Arnell and Gosling, 2014).

We are in a period with a greater incidence of extreme rainfall events (e.g., Coumou and Rahmstorf, 2012; de Leeuw et al., 2015) and model projections indicate further intensification through the current century (e.g., Westra et al., 2014). As a result, quantifying the direct impact of more intense storms on flood behaviour (for subsurface-dominated systems and wider), should be an urgent research priority.

Acknowledgments

The detailed results for this paper are given in the supplementary material, and all data are available by request to the corresponding author. The key stimulus for this modelling work arose from several discussions between N.A.C. and M. Bonell on the role of storm-type in the regulation of hydrograph shape. J. Lancaster is thanked for the collection of the Greenholes basin data when at Lancaster University; M. Bonell for the South Creek data when at James Cook University; Y. Bahat and colleagues at ATREE for the Saimane data; and J. Hanapi of the Yayasan Sabah Group for the Baru data. K. Beven, C.N. Hewitt and P.C. Young of Lancaster University together with the four anonymous reviewers are thanked for their constructive comments. This work was supported by NERC grant WGhats-Capacity (NE/I022450/1) within the NERC Changing Water Cycle programme (in collaboration with Dundee University).

Appendix A. Supplementary data

Supplementary data related to this article can be found at http://dx.doi.org/10.1016/j.envsoft.2016.10.009.

References

Ali, M., Fiori, A., Bellotti, G., 2012. Analysis of the nonlinear storage-discharge relation for hillslopes through 2D numerical modelling. Hydrol. Process. 27, 2683–2690.
Arnell, N.W., Gosling, S.N., 2014. The impacts of climate change on river flood risk at the global scale. Clim. Chang. http://dx.doi.org/10.1007/s10584-014-1084-5.
Barnes, B.S., 1939. The structure of discharge recession curves. Trans. Am. Geophys. Union 4, 721–725.
Bear, J., Zaslavsky, D., Irmay, S., 1968. Physical Principles of Water Percolation and Seepage. Unesco, Paris, France.
Bell, J., 2005. The Soil Hydrology of the Plynlimon Catchments. Institute of Hydrology, Wallingford, U.K.
Beven, K.J., 2012. Rainfall-runoff Modelling: the Primer, second ed. Wiley, Chichester.
Beven, K.J., Germann, P.F., 2013. Macropores and water flow in soils revisited. Water Resour. Res. 49, 3071–3092.
Beven, K., Young, P., 2013. A guide to good practice in modeling semantics for authors and referees. Water Resour. Res. 49, 5092–5098.
Beven, K., Smith, P., 2014. Concepts of information content and likelihood in parameter calibration for hydrological simulation models. J. Hydrol. Eng. A4014010. http://dx.doi.org/10.1061/(ASCE)HE.1943-5584.0000991.
Bidin, K., Chappell, N.A., 2006. Characteristics of rain-events at an inland locality in Northeastern Borneo. Hydrol. Process. 20, 3835–3850.
Bonell, M., Purandara, B.K., Venkatesh, B., Krishnaswamy, J., Acharya, H.A.K., Jayakumar, R., Singh, U.V., Chappell, N., 2010. The impact of forest use and reforestation on soil hydraulic conductivity in the Western Ghats of India: implications for surface and sub-surface hydrology. J. Hydrol. 391, 47–62.
Box, G.E.P., Jenkins, G.M., Reinsel, G.C., 2008. Time Series Analysis: Forecasting and Control. Wiley, Hoboken, U.S.A.
Bren, L.J., Farrell, P.W., Leitch, C.J., 1987. Use of weighted integral variables to determine the relation between rainfall intensity and storm flow and peak flow generation. Water Resour. Res. 23, 1320–1326.
Brommer, D.M., Cerveny, R.S., Balling Jr., R.C., 2007. Characteristics of long-duration precipitation events across the United States. Geophys. Res. Lett. 34, L22712. http://dx.doi.org/10.1029/2007GL031808.
Chappell, N.A., Lancaster, J.W., 2007. Comparison of methodological uncertainty within permeability measurements. Hydrol. Process. 21, 2504–2514.
Chappell, N.A., Ternan, J.L., Bidin, K., 1999. Correlation of physicochemical properties and sub-erosional landforms with aggregate stability variations in a tropical Ultisol disturbed by forestry operations. Soil Till. Res. 50, 55–71.
Chappell, N.A., Tych, W., Chotai, A., Bidin, K., Sinun, W., Thang, H.C., 2006. BARUMODEL: combined Data Based Mechanistic models of runoff response in a managed rainforest catchment. For. Ecol. Manag. 224, 58–80.
Chappell, N.A., Bonell, M., Barnes, C.J., Tych, W., 2012. Tropical cyclone effects on rapid runoff responses: quantifying with new continuous-time transfer function models. In: Webb, A.A., Bonell, M., Bren, L., Lane, P.N.J., McGuire, D., Neary, D.G., Nettles, J., Scott, D.F., Stednik, J., Wang, Y., pp82-93 (Eds.), Revisiting Experimental Catchment Studies in Forest Hydrology (IAHS Publication 353). IAHS Press, Wallingford, U.K.
Coumou, D., Rahmstorf, S., 2012. A decade of weather extremes. Nat. Clim. Change 2, 491–496. http://dx.doi.org/10.1038/nclimate1452.
de Leeuw, J., Methven, J., Blackburn, M., 2015. Variability and trends in England and Wales precipitation. Int. J. Climatol. http://dx.doi.org/10.1002/joc.4521.
FAO-UNESCO, 2004. Digital Soil Map of the World and Derived Soil Properties. FAO, Rome.
Francis, P.A., Gadgil, S., 2006. Intense rainfall events over the west coast of India. Meteorol. Atmos. Phys. 94, 27–42.
Graham, C.B., van Verseveld, W., Barnard, H.R., McDonnell, J.J., 2010. Estimating the deep seepage component of the hillslope and catchment water balance within a measurement uncertainty framework. Hydrol. Process. 24, 3631–3647.
Gregory, K.J., Walling, D.E., 1973. Drainage Basin Form and Process. Edward Arnold, London.

Gilmour, D.A., Bonell, M., Sinclair, D.F., 1980. An investigation of storm drainage processes in a tropical rainforest catchment. In: Aust. Water Res. Council Tech. Pap. 56. Aust. Govt. Pub. Ser, Canberra.
Hand, W.H., Fox, N.I., Collier, C.G., 2004. A study of twentieth-century extreme rainfall events in the United Kingdom with implications for forecasting. Met. Apps. 11, 15–31.
Hewlett, J.D., Fortson, J.C., Cunningham, G.B., 1977. The effect of rainfall intensity on storm flow and peak discharge from forest land. Water Resour. Res. 13, 259–266.
Howard, A., Bonell, M., Cassells, D.S., Gilmour, D.A., 2010. Is rainfall intensity significant in the rainfall-runoff process within tropical rainforests of north-east Queensland? : the Hewlett regression analyses revisited. Hydrol. Process. 24, 2520–2537.
Hugenschmidt, C., Ingwersen, J., Sangchan, W., Sukvanachaikul, Y., Duffner, A., Uhlenbrook, S., Streck, T., 2014. A three-component hydrograph separation based on geochemical tracers in a tropical mountainous headwater catchment in northern Thailand. Hydrol. Earth Syst. Sci. 18, 525–537.
Jakeman, A.J., Hornberger, G.M., 1993. How much complexity is warranted in a rainfall-runoff model? Water Resour. Res. 29, 2637–2649.
Jakeman, A.J., Littlewood, I.G., Whitehead, P.G., 1990. Computation of the instantaneous unit hydrograph and identifiable component flows with application to two small upland catchments. J. Hydrol. 117, 275–300.
Jakeman, A.J., Littlewood, I.G., Whitehead, P.G., 1993. An assessment of the dynamic response characteristics of streamflow in the Balquhidder catchments. J. Hydrol. 145 (3–4), 337–355.
Jones, T.D., Chappell, N.A., 2014. Streamflow and hydrogen ion interrelationships identified using Data-Based Mechanistic modelling of high frequency observations through contiguous storms. Hydrol. Res. 45, 868–892.
Jones, T.D., Chappell, N.A., Tych, W., 2014. First dynamic model of dissolved organic carbon derived directly from high frequency observations through contiguous storms. Environ. Sci. Technol. 48, 13289–13297.
Klingaman, N.P., 2012. A Literature Survey of Key Rainfall Drivers in Queensland, Australia: Rainfall Variability and Change. QCCCE Research Report: Rainfall in Queensland. Part 1, Department of Environmental and Resource Management. Queensland Government, Australia.
Kretzschmar, A., Tych, W., Chappell, N.A., 2014. Reversing hydrology: estimation of sub-hourly rainfall time-series from streamflow. Environ. Modell. Softw. 60, 290–301.
Krishnaswamy, J., Bonell, M., Venkatesh, B., Purandara, B.K., Lele, S., Kiran, M.C., Reddy, V., Badiger, S., Rakesh, K.N., 2012. The rain–runoff response of tropical humid forest ecosystems to use and reforestation in the Western Ghats of India. J. Hydrol. 472, 216–237.
Kundzewicz, Z.W., Napiórkowski, J.J., 1986. Nonlinear models of dynamic hydrology. Hydrol. Sci. J. 31, 163–185.
Lesack, L.F.W., 1993. Water balance and hydrologic characteristics of a rainforest catchment in the central Amazon Basin. Water Resour. Res. 29, 759–773.
Little, M.A., Rodda, H.J.E., McSharry, P.E., 2008. Bayesian objective classification of extreme UK daily rainfall for flood risk applications. Hydrol. Earth Syst. Sci. Discuss. 5, 3033–3060.
Littlewood, I.G., Clarke, R.T., Collischonn, W., Croke, B.F.W., 2007. Predicting daily streamflow using rainfall forecasts, a simple loss module and unit hydrographs: two Brazilian catchments. Environ. Modell. Softw. 22, 1229–1239.
Littlewood, I., Croke, B., 2013. Effects of data time-step on the accuracy of calibrated rainfall-streamflow model parameters: practical aspects of uncertainty reduction. Hydrol. Res. 44, 430–440. http://dx.doi.org/10.2166/nh.2012.099.
Loague, K.M., Freeze, R.A., 1985. A comparison of rainfall-runoff modelling techniques on small upland catchments. Water Resour. Res. 21, 229–240.
McIntyre, N., Young, P., Orellana, B., Marshall, M., Reynolds, B., Wheater, H., 2011. Identification of nonlinearity in rainfall-flow response using data-based mechanistic modeling. Water Resour. Res. 47 http://dx.doi.org/10.1029/2010RW009851.
Merz, R., Blöschl, G., 2003. A process typology of regional floods. Water Resour. Res. 39, 1340. http://dx.doi.org/10.1029/2002WR001952.
Minshall, N.E., 1960. Predicting storm runoff on small experimental watersheds. Proc. Am. Soc. Civ. Eng. 86, 28–33.
Newson, M.D., 1976. The Physiography, Deposits and Vegetation of the Plynlimon Catchments. Report Number 30. Institute of Hydrology, Wallingford.
Noguchi, S., Abdul Rahim, N., Baharuddin, K., Tani, M., Sammori, T., Morisada, K., 1997. Soil physical properties and preferential flow pathways in a tropical rain forest, Bukit Tarek, Peninsular Malaysia. J. For. Res. 2, 115–120.
Ockenden, M.C., Chappell, N.A., 2011. Identification of the dominant runoff pathways from the data-based mechanistic modelling of nested catchments in temperate UK. J. Hydrol. 402, 71–79.
Pedregal, D.J., Rivas, R., Feliu, V., Sánchez, L., Linares, A., 2009. A non-linear forecasting system for the Ebro River at Zaragoza, Spain. Environ. Modell. Softw. 24, 502–509.
Peel, M.C., Finlayson, B.L., McMahon, T.A., 2007. Updated world map of the Köppen-Geiger climate classification. Hydrol. Earth Syst. Sc. 11, 1633–1644.
Reynolds, B., Norris, D.A., 1990. Llyn Brianne Acid Waters Project – Summary of Catchment Characteristics. Institute of Terrestrial Ecology, Bangor.
Rodríguez-Iturbe, I., Gonzales-Sanabria, M., Camano, G., 1982. On the climatic dependence of the IUH: a rainfall-runoff theory of the Nash model and the geomorphoclimatic theory. Water Resour. Res. 18, 887–903.
Saidi, H., Ciampittiello, M., Dresti, C., 2014. Extreme rainfall events: evaluation with different instruments and measurement reliability. Environ. Earth Sci. 72, 4607–4616.
Seibert, J., Beven, K.J., 2009. Gauging the ungauged basin: how many discharge measurements are needed? Hydrol. Earth Syst. Sc. 13, 883–892.
Shepherd, J.M., Grundstein, A., Mote, T., 2007. Quantifying the contribution of tropical cyclones to extreme rainfall along the coastal southeastern United States. Geophys. Res. Lett. 34, L23810. http://dx.doi.org/10.1029/2007GL031694.
Sherman, L.K., 1932. Streamflow from rainfall by unit-graph method. Eng. News Rec. 108, 501–505.
Taylor, C.J., Pedregal, D.J., Young, P.C., Tych, W., 2007. Environmental time series analysis and forecasting with the Captain toolbox. Environ. Modell. Softw. 22, 797–814.
Wang, C.T., Gupta, V.K., Waymire, E., 1981. A geomorphologic synthesis of nonlinearity in surface runoff. Water Resour. Res. 17, 343–554.
Weiler, M., 2005. An infiltration model based on flow variability in macropores: development, sensitivity analysis and applications. J. Hydrol. 310, 294–315 (2005).
Westra, S., Fowler, H.J., Evans, J.P., Alexander, L.V., Berg, P., Johnson, F., Kendon, E.J., Lenderink, G., Roberts, N.M., 2014. Future changes to the intensity and frequency of short-duration extreme rainfall: future intensity of sub-daily rainfall. Rev. Geophys. 52, 522–555. http://dx.doi.org/10.1002/2014RG000464.
Whitehead, P.G., Young, P.C., Hornberger, G.M., 1979. A systems model of streamflow and water quality in the Bedford-Ouse: 1. Streamflow modelling. Water Resour. Res. 13, 1155–1169.
Wohl, E., Barros, A., Brunsell, N., Chappell, N.A., Coe, M., Giambelluca, T., Goldsmith, S., Harmon, R., Hendrickx, J., Juvik, J., McDonnell, J., Ogden, F., 2012. The hydrology of the humid tropics. Nat. Clim. Change 2, 655–662.
Ye, W., Jakeman, A.J., Young, P.C., 1998. Identification of improved rainfall-runoff models for an ephemeral low-yielding Australian catchment. Environ. Modell. Softw. 13, 59–74.
Young, P., 1998. Data-based mechanistic modelling of environmental, ecological, economic and engineering systems. Environ. Modell. Softw. 13, 105–122.
Young, P.C., 2013. Hypothetico-inductive data-based mechanistic modeling of hydrological systems. Water Resour. Res. 49, 915–935.
Young, P.C., 2015. Refined instrumental variable estimation: maximum likelihood optimization of a unified Box–Jenkins model. Automatica 52, 35–46.
Young, P.C., Jakeman, A.J., 1979. Refined instrumental variable methods of recursive time-series analysis Part I. Single input, single output systems. Int. J. Control 29, 1–30.
Young, P.C., Beven, K.J., 1994. Data-based mechanistic modelling and the rainfall-flow nonlinearity. Environmetrics 5, 335–363.
Young, P.C., Garnier, H., 2006. Identification and estimation of continuous-time, data-based mechanistic (DBM) models for environmental systems. Environ. Modell. Softw. 21, 1055–1072.
Zipser, E.J., Cecil, D.J., Liu, C.T., Nesbitt, S.W., Yorti, D.P., 2006. Where are the most intense thunderstorms on Earth? B. Am. Meteorol. Soc. 87, 1057–1071.